30th AIAA Applied Aerodynamics Conference
25 - 28 June 2012, New Orleans, Louisiana

AIAA 2012-3212

Dominant flow structures in the wake of a cyclist

Timothy N. Crouch[1], Mark Thompson[2], David Burton[3], John Sheridan[4]
Monash University, Clayton, Victoria, 3800 Australia

and

Nicholas A.T. Brown[5]
Australian Institute of Sport, Belconnen, Canberra, 2617 Australia

In this wind tunnel investigation the time-averaged wake structure is analyzed for a full scale cyclist mannequin over a complete crank cycle. At typical elite level road cycling speeds, detailed velocity field measurements were performed by traversing a four-hole dynamic pressure probe in planes behind the mannequin for 15° increments in crank position. They highlight the complexity of flows associated with cyclist geometries and show that variations in drag with leg position are primarily attributed to changes in the flow regime and not frontal surface area. The wake is shown to be highly three-dimensional with the primary flow structures consisting of multiple streamwise vortices. The formation strength and interaction of these structures about the center plane of the mannequin depend on whether each leg is in an up or down position around the crank cycle. This dependence on the position of each leg results in an asymmetrical wake configuration for the majority of crank positions tested. This is further highlighted in a series of flow visualization studies showing the origin and asymmetry in the formation of these structures over the upper body with crank position. This work highlights the importance of considering multiple flow regimes when investigating the aerodynamic performance of cyclists.

Nomenclature

FSA	=	*frontal surface area*
Cd.A	=	*drag area*
Cd	=	*drag coefficient*
θ	=	*crank angle*
Φ	=	*hip angle*
(x,y,z)	=	*wind tunnel coordinate system*
U_∞	=	*free stream reference velocity*
(u,v,w)	=	*components of the local velocity field*
(U,V*,W*)*	=	*normalised local velocity components*
ω_x	=	*streamwise vorticity*
λ_{ci}	=	*swirling strength*

I. Introduction

Over the past two decades cycling has evolved primarily due to the recognition that small reductions in drag can result in large gains in cycling performance. The drive to reduce drag has influenced both the design of the bicycle and rider's equipment as well as the positions employed by cyclists on the bicycle. Of the total resistance experienced by a cyclist, as much as 90% is associated with aerodynamic drag even at relatively low cycling

[1] Graduate Student, Dept. of Mech. & Aero. Eng., Monash University, Victoria, Australia
[2] Head of Department, Dept. of Mech. & Aero. Eng., Monash University, Victoria, Australia
[3] Wind Tunnel Manager, Dept. of Mech. & Aero. Eng., Monash University, Victoria, Australia
[4] Deputy Dean, Dept. of Mech. & Aero. Eng., Monash University, Victoria, Australia, Senior AIAA Member
[5] Deputy Director, Research & Applied Science, Australian Institute of Sport, Canberra, Australia

speeds.[1] Due to the size and bluff body nature of the cyclist's geometry, the majority of this drag is the pressure drag acting on the rider, a consequence of flow separation.

Unlike simple bluff body geometries, a cyclist consists of multiple body parts, all of which are complex curved shapes and all of which can vary significantly between individuals. Add to this the complexities associated with the motion of the rider throughout the pedal stroke and the fluid dynamic problem surrounding cyclist aerodynamics becomes very complicated. This is one of the main reasons why current wind tunnel investigations cannot explain the variation in drag observed between different cyclists and their positions. As a result of this lack of understanding, the most effective way to date to evaluate the aerodynamic performance of rider position and equipment has been through trial and error force measurements in a wind tunnel.

Fundamental to better understanding how drag varies between different cyclists, and how we can efficiently reduce it, is an understanding of the flow structure over the cyclist. Currently, little is known about the overall flow topology around a cyclist. We do not know the location of the large separated flow regions, nor the mechanisms that affect the drag of a cyclist, or how cyclist characteristics/position affects these. Previous investigations into complex bluff body flows, such as in vehicle aerodynamics, have shown that investigating the wake structures can lead to a better understanding of how changes in vehicle geometry can affect the pressure distribution over the body, leading to changes in drag. One of the most influential findings on vehicle shape development has been the identification of streamwise trailing vortices as a dominant feature of vehicle wakes.[2] Due to the restrictions placed on rider attire, position and equipment by the Union Cycliste Internationale, the extent to which the shape of a bicycle and rider system can be changed is limited. However by identifying dominant wake structures, as demonstrated in vehicle aerodynamics, we can start to build an understanding of how different rider shapes and positions affect drag.

In this quasi-steady analysis the time averaged flow structures are identified in the wake of a cycling mannequin and the effect of systematically varying the position of the legs around the crank on wake structure and drag are addressed. In doing so, this research provides a solid foundation for characterizing these complex flows.

II. Experimental Investigations

A range of wind tunnel investigations were performed to identify the dominant flow structures in the wake of a cyclist which predominantly influence drag, and how these are affected by changes to leg position. In order to investigate flow phenomena of rider aerodynamics, a full scale cyclist mannequin was developed. The mannequin ensures repeatability of position and facilitates experimental studies not normally practical with a real rider. Investigations conducted on the mannequin include time averaged drag measurements, wake surveys and flow visualization studies which were performed in two separate wind tunnels. Although experiments were conducted in two wind tunnel environments, collaborated results only strengthen findings surrounding the dominant wake features and the influence of leg position on drag. Results discussing variations in the evolution of the wake throughout the cycle of the crank are limited to a quasi-steady analysis of the wake of the upper body. Further work on the role that cadence plays on the development and shedding characteristics of primary flow structures that determine aerodynamic forces is required. However, given that the ratio of the speed of the legs around a crank cycle to the forward speed of a cyclist is low, even at high cadences, it is expected that outcomes relating to wake evolution with leg position presented in this investigation will be similar to that if the cyclist was in pedaling motion.

A. Mannequin Equipment, Position and Geometry

Figure 1 shows the time-trial position and rider equipment used for the mannequin which was adopted throughout all studies presented in this paper. The position of the mannequin on the bicycle is representative of a typical low-drag time trial position.

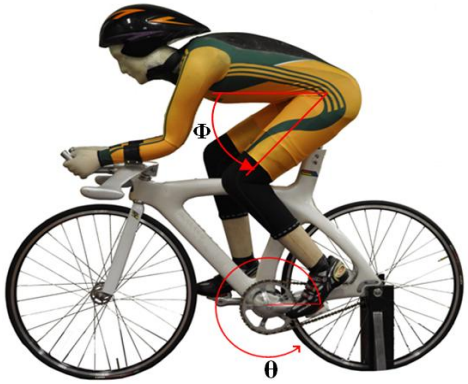

Figure 1. Mannequin position and equipment

Knee and hip joints allow for the legs to rotate about the crank. A braking mechanism was applied to the rear wheel so that leg position could be systematically varied in the forward pedaling direction around the crank cycle. The position of the legs is defined by the angle of the crank where the 0° crank position (shown in Figure 1) is when the crank is horizontal, with the right leg forward and the left leg back. The hip angle of each leg is defined as the angle between the horizontal and the upper leg. To ensure that the characteristic features of the wake are representative of a real cyclist, the mannequin was modeled on a typical male cyclist in a time-trial position. Special attention was placed on

the design of the torso where dominant flow structures are thought to originate. Key geometric features of the mannequin include a standing height of 1.80 m, a torso length of 650mm and a shoulder and hip width of 420 mm and 350 mm respectively.

In addition to the knee, hip and ankle joints that allow the legs to be positioned around the crank the mannequin also has design features that allow for the position of the arms, head, neck and torso to be altered. The flexibility in the positioning of the main body components allows for a wide range of representative cycling positions to be investigated.

B. Force Measurements

Time averaged drag forces of static mannequin leg positions were measured in 15° increments around one complete cycle. Force measurements were conducted in the 3/4 open-jet test section of the large wind tunnel at the Department of Mechanical and Aerospace Engineering, Monash University. The blockage ratio of the mannequin in this test section based on the 2.6 x 4.0 m sectional area at the nozzle exit is approximately 4%. At the free-stream test speed of 16 m/s the turbulence intensity in the middle of the test section, where the mannequin was positioned, is less than 1.6%. Measurements conducted at this free-stream test velocity correspond to a Reynolds number of 6.9 x 10^5 based on the torso length of the mannequin.

The drag force acting on the mannequin and bicycle system was measured using a six-component force balance of the piezoelectric Kistler type that was calibrated prior to force measurements. Struts attached to either side of the front and rear wheel were used to rigidly fix the bicycle and mannequin system to the force balance housed underneath the wind tunnel floor. The mannequin was positioned on a raised box with a cantilevered splitter extending over the leading edge of the platform to limit the impact of the raised box and wind tunnel floor boundary layer on force results.

Force measurements at each crank angle are taken as the mean result of three separate tests sampled at 500 Hz for 30 seconds. The maximum standard deviation between individual tests and the final mean result was less than 0.5% at any given crank angle.

C. Flow Field Measurements

Detailed wake surveys were performed using a four-hole dynamic pressure probe in a plane normal to the mean flow projected behind the upper body of the mannequin, and approximately one torso length (600mm) behind the mannequin as shown in Figure 2. Time averaged sectional flow field measurements were performed in 15° increments around a complete crank cycle. These measurements were conducted in a smaller 450kW closed-loop wind tunnel, with an effective working section of 2.0 x 2.0 m, also located at the Department of Mechanical and Aerospace Engineering, Monash University. The turbulence intensity in this working section is 1.4% with a blockage ratio of 10%.

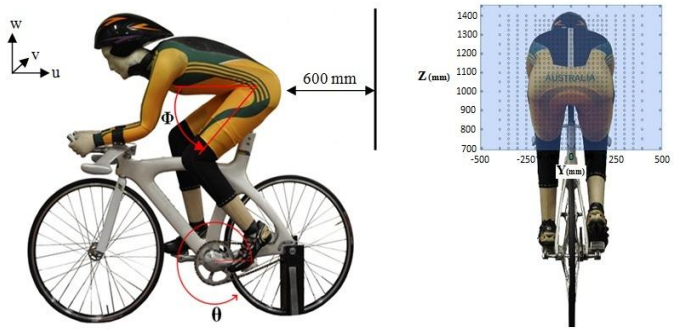

Figure 2. Wake survey traversing plane 600mm into the near wake behind mannequin

The wake surveys are constrained to a partial section of the wake in a 0.75 x 1.0 m plane centered about the central plane of the mannequin, 0.7 m above the wind tunnel floor. The wake surveys consist of probe measurements sampled at 1250 Hz for 15 seconds, at 888 locations in the traverse plane. The probe was traversed to capture the entire wake of the upper body with traverse measurements extending into the flow field that exhibited the same turbulence intensity as the free-stream. Directly behind the mannequin the density of probe measurements was increased in areas of the wake that exhibited large velocity gradients. The vertical and horizontal grid spacing between measurement points in this section of the wake was 25 mm and 20 mm respectively. A second probe located in the free-stream, 3.0 m upstream of the mannequin, was also used as a reference. Reference probe measurements were recorded simultaneously throughout the duration of each traverse measurement and used to normalize any velocity or density variations over the duration of a traverse.

D. Flow Visualization Methods

Smoke flow visualization tests were conducted in the 3/4 open-jet test section of the large Monash wind tunnel at a free stream velocity of approximately 10 m/s. Smoke was injected at various points around the body of the

mannequin highlighting the evolution of flow structures as the position of the legs were systematically varied around the crank. These visualizations were simultaneously recorded on video footage from three cameras that were positioned above, side and rear views of the mannequin.

III. Results

A. Force Measurements

Figure 3 shows the measured variation in drag determined at 15° increments in crank position for one complete crank cycle. It is apparent that the position of the legs around the crank has a large effect on the force, with a 20% variation in drag over the cycle.

The results for the two halves of the cycle agree well, with a maximum variation in opposite leg positions of less than 5%. Both halves of the cycle show that the drag does not change significantly over the first 15° rotation of the crank, and then increases rapidly until it reaches a maximum at the 75° and 255° crank positions. Following the peak in drag, in both halves of the cycle the drag decreases but at a reduced rate compared to that at which it increased. It can be seen that over the range of crank angles where the drag reduces that there is a more rapid reduction near the end of this range. The high repeatability of force measurements, along with traverse results to be discussed later, suggest that the difference in drag is a physical property of the mannequin possibly due to slight asymmetries in its geometry and position. These minor variations between opposite leg positions do not compromise the overall conclusions drawn, and we assume one half of the crank cycle to be representative of the data trend.

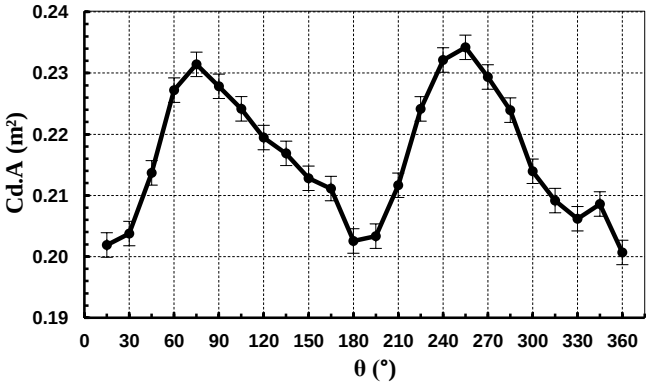

Figure 3. Variation in drag area over a complete crank cycle

In an attempt to explain the large variation in drag with changes in leg position, the combined frontal surface area of the mannequin and bicycle system was determined at each crank angle where force measurements were recorded. The frontal area was determined from photographs taken from 10 m in front of the mannequin, with a reference area held at the mid-point of the crank. Frontal area was then calculated by counting photograph pixels within the boundaries of the mannequin and the bicycle. Figure 4a shows that the variation in frontal area due to a change in leg position is less than 2% over a complete cycle of the crank. Although the frontal surface area maxima and minima coincide with the low and high drag crank positions, the small change in frontal area cannot account for the large variation in drag.

By taking into account the effect that changes in the total frontal area have on the drag and extracting them out of the Cd.A values, we obtain Figure 4b, which shows that the variations in drag are primarily due to the drag

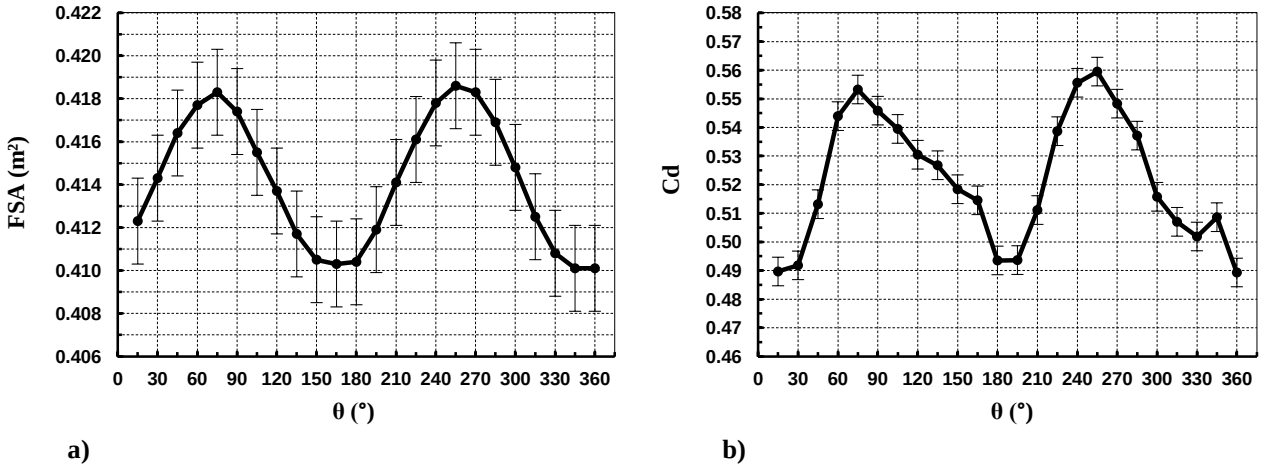

Figure 4. Change in frontal surface area (a) and drag coefficient (b) with crank angle

coefficient. The large change in the drag coefficient (up to 15%) suggests that as the legs are moved around the crank, there is a large change in the flow regime over the mannequin. The sectional wake surveys show this to be the case and that the variation in drag with leg position is a result of a change in the flow structure and not frontal surface area.

B. Flow Field Measurements

Traverse results reveal how variations in the position of the legs results in a change in the flow regime, and that dominant features of the wake having the greatest impact on drag are highly dependent on leg position Figure 6 and

Figure 7 show time averaged contour plots of the streamwise velocity and vorticity fields with the in plane velocity vector components overlaid for all traversed crank angles. The wake traverses show large variations in the size and shape of the wake over the crank cycle, highlighting the degree to which leg position affects the flow.

The wake surveys conducted in the small wind tunnel are in good agreement with force measurements conducted in the larger wind tunnel. A wake integral analysis was performed on the sectional velocity field data yielding an approximation of the drag that could be compared with the force measurements, which is shown in Figure 5. The integral method used, commonly referred to as Maskell's approach, consists of three integral terms that account for defects in wake stagnation pressure, streamwise velocity and the drag associated with the in plane cross flow components, commonly referred to as vortex drag.[3] This control volume approach results in an approximation of the drag that excludes unsteady effects. As expected, due to the partial traverse of the wake and the limitations of Maskell's approach, the absolute value of the drag approximated from the sectional velocity field measurements is lower than the measured force results. However the difference in drag results between the two methods is relatively constant showing that the overarching trends between drag and leg position compare very well regardless of the method used. Both methods identify the same maximum and minimum drag cases occurring at 75° and 0° to 15° respectively. They both show similar minor variations in force measurements between opposite leg positions, previously discussed in the Kistler force measurement section, suggesting that these differences are a physical feature of the mannequin.

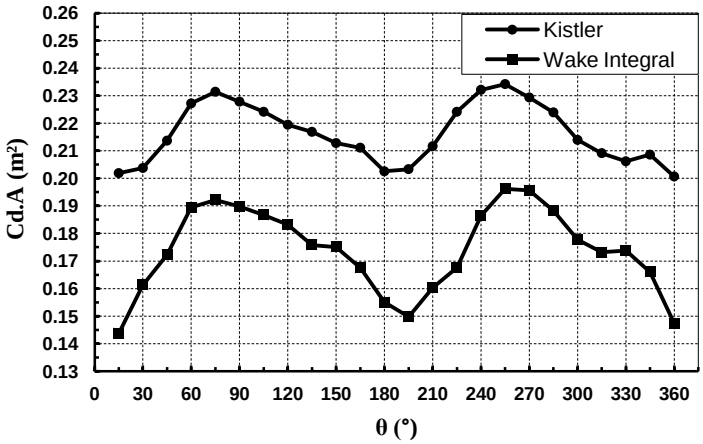

Figure 5. Comparison of measured drag results (Kistler) with the wake integral drag approximation

The similar variation in drag with leg position suggests that the principle flow structures causing this variation have been captured within the section of the wake analyzed over the upper body. The similarities in the effect of leg position on drag between the two separate studies also suggests that the principle flow mechanisms and structures that determine the drag were consistent in both wind tunnel studies. Conclusions drawn on the mechanisms and flow structures that determine the drag of a cyclist are therefore not expected to have been significantly influenced by the separate wind tunnels and the effects of the higher blockage ratio of the smaller tunnel.

The time averaged contours of streamwise velocity reveal that both halves of the cycle show two dominant features of the wake, an asymmetrical (high drag) and symmetrical (low drag) flow regime. For the majority of crank angles the wake is asymmetrical, showing the flow varies significantly about the center plane of the mannequin depending on leg position. At the 15° and 195° crank positions which correspond to the point at which the left and right thighs are in line with each other ($\Phi_{LEFT} = \Phi_{RIGHT}$), the wake is symmetrical about the center plane and as the legs are moved around the cycle the wake progressively transitions to the asymmetrical flow regime. The high drag asymmetrical case is characterized by regions of high streamwise velocity over the hips on the side of the body with the leg in a raised position, and regions of reduced velocity over the hips on the opposite lowered side, that extend down into both sides of the lower wake.

The asymmetry in the flow pattern results from a variation in the location at which the flow separates from the left and right sides of the body. This can be observed in Figure 6, for all crank angles other than 0°, 15°, 180° and 195°. The flow remains attached over the hips in the upward leg position, as indicated by the regions of higher streamwise velocity, while the low streamwise velocity region extending high up on the hip in the downward leg

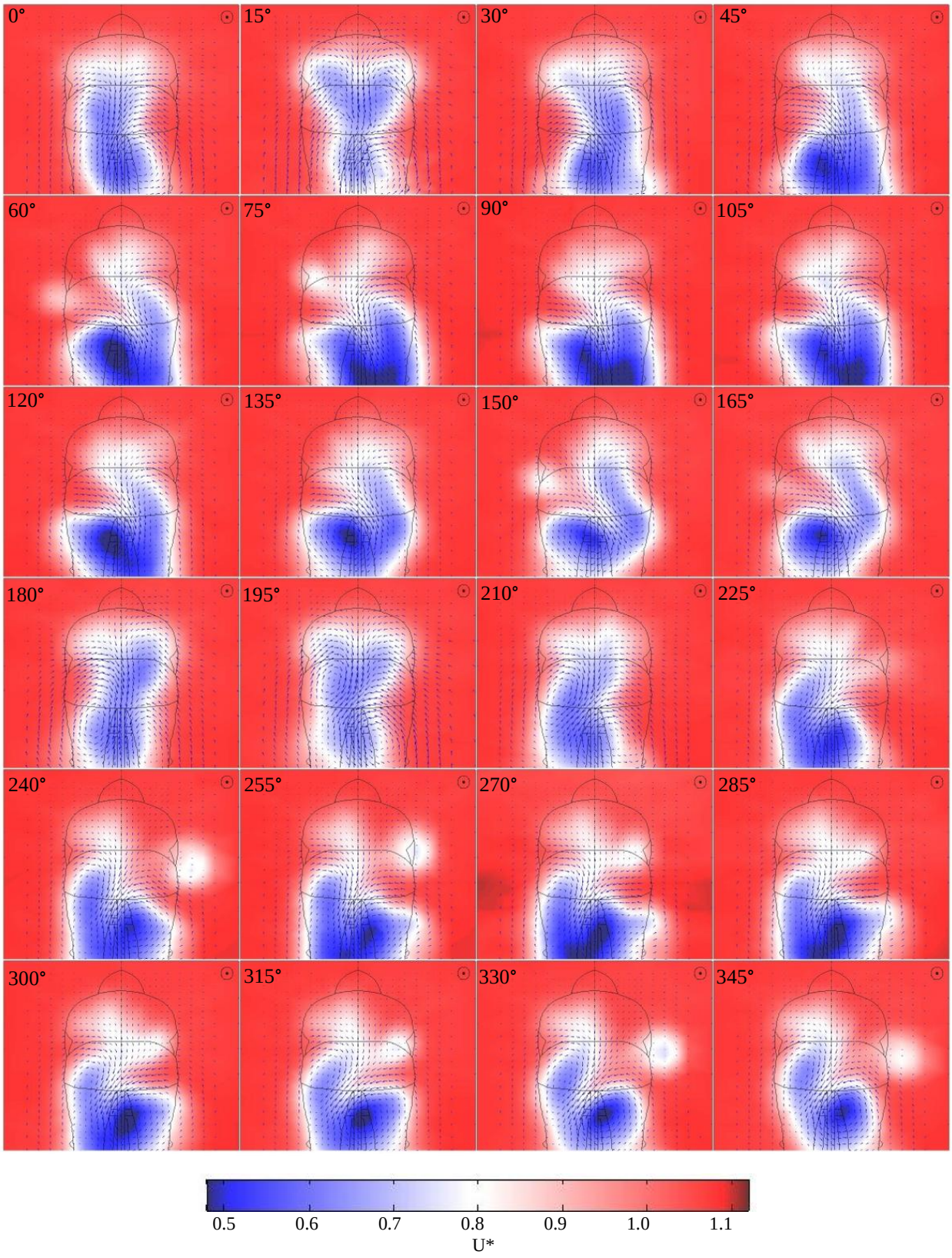

Figure 6. Streamwise velocity field U* = u/U∞ in the traverse plane 600mm behind the mannequin

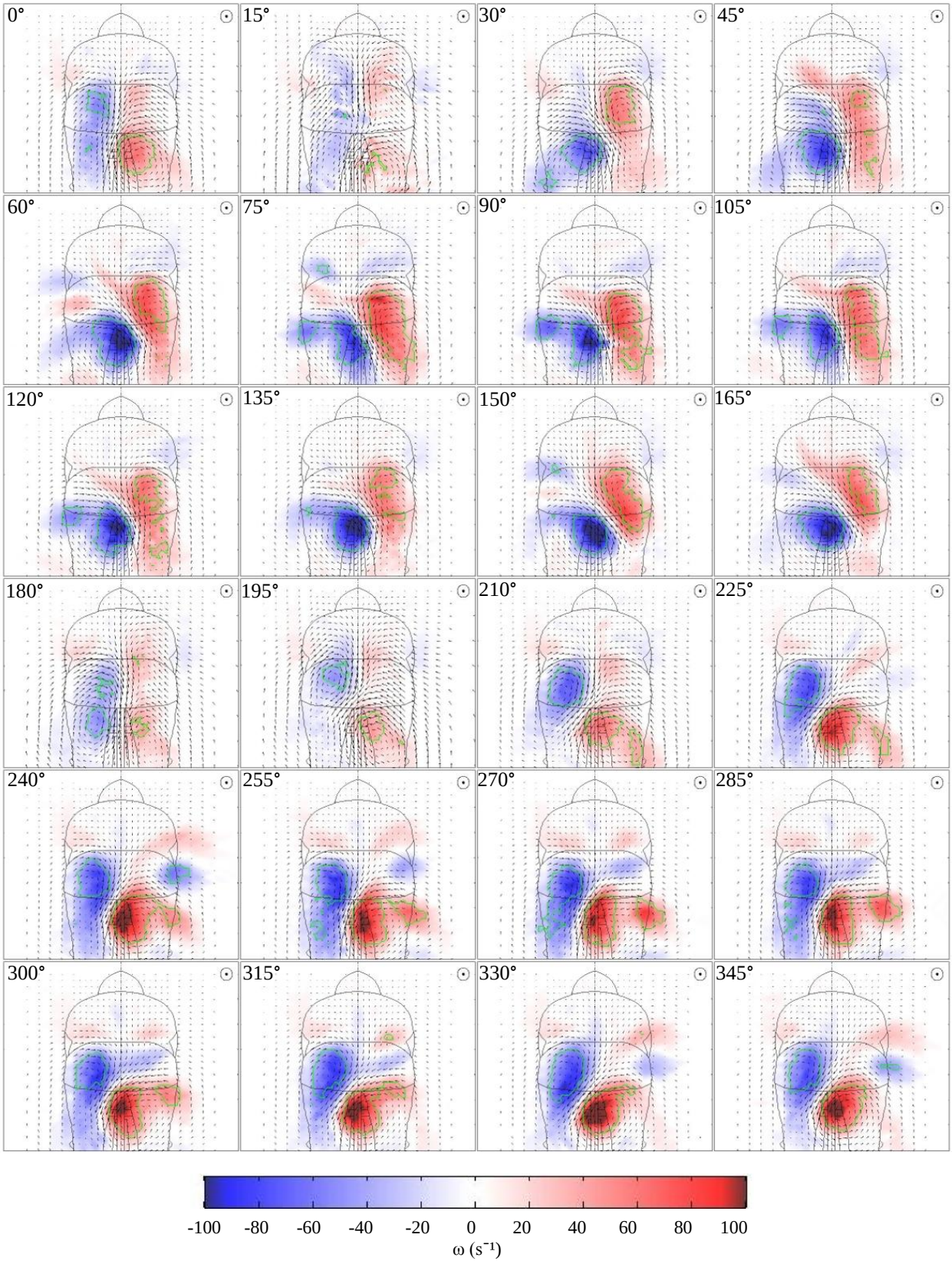

Figure 7. Streamwise vorticity field in the traverse plane 600mm behind the mannequin

positions shows that the flow is separated. For the low drag symmetrical case the flow is observed to separate high on both hips resulting in an increase in the size of the wake above them. However this also results in a significant reduction in the size and magnitude of the separated regions below the hips where the majority of the drag originates, resulting in reduced overall drag.

Contours of vorticity reveal that the low velocity separated regions that determine the drag are characterized by regions of high vorticity. This demonstrates how the primary features of the wake consist of streamwise vortex structures. Figure 7 shows contours of vorticity at each crank angle with the dominant vortex structures outlined. Vortex structures are identified using the swirling strength criterion, which measures the significance of vortical structures based on the imaginary part λ_{ci} of the complex eigenpairs of the velocity gradient tensor derived from critical point analysis.[4] Vortex structures in the wake of the mannequin were characterized as regions of λ_{ci}^2 being above a threshold level that was set as the square of the maximum swirling strength determined from an empty wind tunnel traverse across the test section.

A large pair of streamwise counter rotating (lifting) vortices of unequal strength can be seen to be the primary features of the wake. These structures are analogous to vortex structures formed over low aspect ratio wings due to a pressure differential created between the lower and upper wing surfaces. In a similar manner, vortex structures identified in the wake of the mannequin are generated due to pressure gradients between the underside of the torso and the hips/lower back region where the primary structures originate from.

The impact of the leg position on the formation and strength of these primary structures is significant throughout a complete cycle of the crank. Similar to the flow regimes identified in Figure 6, Figure 7 identifies a symmetrical flow regime characterized by low vorticity and an asymmetrical regime where the primary vortex pair dominates the wake. The relative strength and spatial coherence of vortex structures from the left and right sides of the body change depending on the position of the legs. The stronger of the pair is generated due to the separated flow rolling up from the base of the hips and between the legs, whereas the weaker and more elongated of the pair is a result of the flow separation from high on the hips.

The asymmetry in the location of flow separation results in the main vortex pair being skewed in both the vertical and horizontal directions of the wake. This is clearly shown in Figure 8, which demonstrates the spatial development of vortices in the traverse plane with changes in leg position. This is represented as iso-surfaces of regions of high vorticity within the boundary of vortex regions identified by the swirling strength criterion. From the different perspectives provided by these iso-surfaces, a clear understanding of how the vortex structures in the wake evolve and transition throughout the crank cycle is evident. The location of primary vortex structures originating

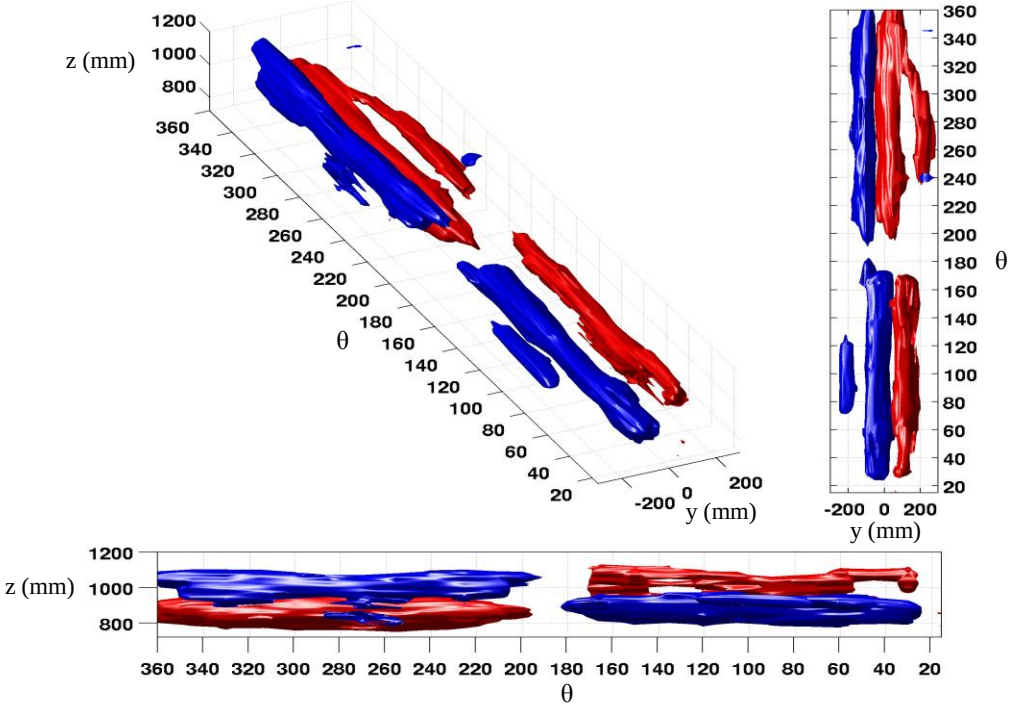

Figure 8. Swirl-Iso surfaces coloured by vorticity. Red is positive and blue is negative

from each side of the body alternate between a low position in the wake on the side of the body, when the leg is in an upward position, to a higher position in the wake, when the leg is in the downward position. The lower and stronger of the vortex pair is also located close to the center plane of the mannequin in the wake with the higher positioned vortex separating further out on the hips. The asymmetrical orientation of the primary vortex pair results in the flow being strongly yawed across the hip of the upward leg and the down-wash created by these vortices being directed across the plane of symmetry in the wake.

A smaller streamwise vortex structure, of the same sign as the large vortex in between the legs, is also identified in each half of the crank cycle. This vortex is formed when flow originating between the legs separates from the inner thigh of the leg that is rising to meet the stomach. Interaction with this secondary structure and the dominant pair can be seen due to the near proximity of the structures in the wake. Figure 6 and Figure 7also indicate further interaction with the primary vortex pair and separated flow originating further upstream. These separated regions are likely to have originated from the arms and helmet which interact with the primary structures in the wake. This further highlights the complexity associated with cycling aerodynamics and that the position of the leg has a large influence on the flow over the entire body of the mannequin.

C. Flow Visualizations

Flow visualization used smoke to view the off-body and near wake flow. The results are consistent with the findings from the sectional flow field data in the wake despite the lower free stream velocity. Changes in the flow pattern that were observed as leg position was varied are consistent with findings from the sectional wake surveys that indentify structures in the wake that dominate the flow field. The smoke particle trajectories clearly identify the influence of leg position on the major fluid mechanisms that lead to both the symmetrical and asymmetrical flow regimes. Flow visualizations also highlight that the asymmetry of the flow over the mannequin is not constrained to just the hips and lower back region with the flow over the entire torso being affected. Flow visualizations reinforce previous findings that show the measured variation in drag over a crank cycle is primarily caused by a change in the flow structure over the mannequin and is not a result of an increase in frontal area.

Figure 9 shows the low drag symmetrical flow regime for the 15° crank angle position when the thighs are aligned. Smoke particles injected into the flow close to the body just in front of the hips shows that the flow comes up from chest of the mannequin and separates evenly across both upper hips. This results in the smoke particles taking an upwards trajectory into the wake.

Smoke injected into the same region for the 240° crank position, representing an example of the asymmetrical flow regime, shows the asymmetry in flow separation from the hip in the upward leg position and the hip in the downward leg position. Smoke particles injected onto the left side of the body where the leg is in a down position shown in Figure 10a show the smoke particles following an upwards trajectory into the wake and over the left hip revealing that the flow separates on the side of the torso and upper hips due to the flow sweeping up from beneath the torso. In contrast to this, smoke particles injected over the right hip, where the leg is in an upwards position, as in Figure 10b, show a downward path into the near wake. The smoke particles show that the flow is attached over this hip, where they follow a path from the edge of the hip in towards the center of the mannequin where the flow then separates and rolls up into the vortex formed at the base of the lower back and in between the legs.

a) **b)**

Figure 9. Smoke injected over the left (a) and right (b) hips for θ = 15°

a)

b)

Figure 10. Smoke visualization from side and rear views showing asymmetry in flow separation over left (a) and right (b) hips for θ = 270°

IV. Conclusion

This investigation analyzed the primary causes of large variations in drag measured on a cyclist mannequin for varying leg positions. It was found that changes in frontal area alone could not explain the large variations in drag throughout the crank cycle, which were primarily attributed to a change in the drag coefficient. Time averaged flow field measurements in the wake of the mannequin demonstrated the extent to which leg position influences the flow, and identified the dominant flow structures that determine drag. The wake is characterized by a pair of strong counter rotating trailing vortices. The formation, strength and orientation of these primary structures is dependent on leg position. A quasi-steady analysis of the evolution of these structures in the wake shows two primary flow regimes. One, symmetrical low drag regime associated with the cycle of the crank when the upper thighs are in line and another, asymmetrical high drag regime when the legs are in an up down position around the crank. In characterizing the dominant wake structures of the mannequin a solid foundation is formed for explaining the effect of rider shape and position on drag. These results show that the flow around a cyclist is very complex and that multiple flow regimes must be considered when optimizing rider aerodynamics.

Acknowledgments

This research was partially supported under Australian Research Council's Linkage Projects funding scheme (project number LP100200090).

References

[1]Kyle, C. R., and Burk, E. R., "Improving the racing bicycle," *Mechanical Engineering*, Vol. 105, No. 9, 1984, pp. 34-35.

[2]Ahmed, S.R., and Ramm, G., "Some Salient Features of the Time-Averaged Ground Vehicle Wake," *SAE Technical Paper 840300*, 1984

[3]Maskell, E., "Progress towards a method for the measurement of the components of the drag of a wing of finite span," Royal Aircraft Establishment Technical Report No. 72232, 1973

[4]Zhou, J., Adrian, R.J., Balachander, S., and Kendall, T.M.., "Mechanisms for generating coherent packets of hairpin vortices in channel flow," *Journal of Fluid Mechanics*, Vol. 387, 1999, pp. 353-396.